Molecular MALDI Imaging: An Emerging Technology for Neuroscience Studies

Maxence Wisztorski,[1] Dominique Croix,[1] Eduardo Macagno,[2] Isabelle Fournier,[1] Michel Salzet[1]

[1] Laboratoire de Neuroimmunologie des Annélides, FRE CNRS 2933, Équipe Imagerie MALDI, Cité Scientifique, Université des Sciences et Technologies de Lille, 59650 Villeneuve d'Ascq, France

[2] Section of Cell and Developmental Biology, Division of Biological Sciences, University of California, San Diego, La Jolla, California 92093

Received 18 September 2007; revised 17 December 2007; accepted 23 December 2007

ABSTRACT: **Mass spectrometry (MS) has become an essential tool for the detection, identification, and characterization of the molecular components of biological processes, such as those responsible for the dynamic properties of the nervous system. Generally, the application of these powerful techniques requires the destruction of the specimen under study, but recent technological advances have made it possible to apply the matrix-assisted laser desorption/ionization (MALDI) MS technique directly to tissue sections. The major advantage of direct MALDI analysis is that it enables the acquisition of local molecular expression profiles, while maintaining the topographic integrity of the tissue and avoiding time-consuming extraction, purification, and separation steps, which have the potential for introducing artifacts. With automation and the ability to display complex spectral data using imaging software, it is now possible to create multiple 2D maps of selected biomolecules in register with tissue sections, a method now known as MALDI Imaging, or MSI (for Mass Spectrometry Imaging). This creates, for example, an opportunity to correlate functional states, determined *a priori* with live recording or imaging, with the corresponding molecular maps obtained at the time the tissue is frozen and analyzed with MSI. We review the increasing application of MALDI Imaging to the analysis of molecular distributions of proteins and peptides in nervous tissues of both vertebrates and invertebrates, focusing in particular on recent studies of neurodegenerative diseases and early efforts to implement assays of neuronal development.** Develop Neurobiol 68: 845–858, 2008

Keywords: **mass spectrometric imaging; MALDI imaging; proteomics; nervous system; neuro-development**

INTRODUCTION

Our understanding of the properties of living systems has increased tremendously since the invention of optical microscopy, as novel tools and ever more powerful methods have been introduced and applied to the acquisition of increasingly detailed morphological and functional information. For instance, without taking anything away from Cajal's formidable ability to discern—correctly for the most part—developmental and functional properties of the neural growth cone from fixed preparations of Golgi stained embryonic brains, it is evident that our current ability to

Correspondence to: E. Macagno (emacagno@ucsd.edu).

Contract grant sponsor: Ministère de L'Education Nationale, de L'Enseignement Supérieur et de la Recherche, ACI Jeunes Chercheurs; contract grant number: ACI JC4074.

Contract grant sponsors: Centre National de la Recherche Scientifique Département de la Politique Industrielle; Agence National de la Recherche, Institut National du Cancer; U.S. National Science Foundation and U.S. National Institutes of Health.

Published online 28 March 2008 in Wiley InterScience (www.interscience.wiley.com).
DOI 10.1002/dneu.20623

make real-time observations at the molecular level in live embryos has greatly enhanced our understanding of how a growth cone navigates through complex environments to reach, recognize, and innervate a target. Dynamic functional imaging applied to the nervous system, the general theme of this special issue of Developmental Neurobiology, can now provide exquisitely accurate spatiotemporal data of signaling events occurring at both the supracellular and subcellular levels in live neurons and neural tissues, *in vitro* and *in vivo*. In parallel, more powerful molecular biological techniques, and their application to the sequencing of the human and other genomes, have given rise to the fields of genomics and transcriptomics which, coupled with great advances in mass spectrometry (MS) and proteomics, are beginning to provide superbly detailed data on the molecular underpinnings of specific cellular functions.

Arguably, a full understanding of neural function will require that we incorporate into our explanations specific, systems-level information about the location, abundance, and physiological states of all functionally important proteins, such as ion channels and neurotransmitter receptors, peptides, and other small molecules that are critically involved in intracellular and intercellular signaling, and other molecules involved in neural functions. Such data can be of great value in the formulation of realistic predictive models, constraining the ranges of key variables that are used in the model and defining the level of structural noise that must be accounted for in achieving functional states that yield consistent behavioral outputs within a species. Thus, we felt it would be useful to contribute here, among reviews of dynamic functional imaging, a review of a recent application of MS to the direct acquisition of complete data on the distribution and abundance of proteins and peptides in neural tissues.

MASS SPECTROMETRY IMAGING (MSI)

Improvements in MS instrumentation and methodologies have made MS the technique of choice for the identification and characterization of biomolecules, particularly in proteomic studies. Generally, proteomic studies require homogenization of a sample as well as long, often tedious and time-consuming extraction, purification, and separation steps before molecular characterization is performed, mostly without preserving anatomical information to correlate location in the tissue with expression profiles of particular peptides and proteins (Aebersold and Goodlett, 2001). However, over the past decade, a new application of a widely used technology, matrix-assisted laser desorption/ionization (MALDI) MS, has been increasingly used to assay molecular profiles directly from frozen or preserved tissue slices, reducing the number of preparative steps, while preserving topographical information about molecular distributions and localization (Chaurand et al., 1999; Fournier et al., 2003).

Basically, in this scanning-mode application of MALDI-MS, series of pulses of a focused laser beam are directed at predetermined positions in a tissue slice that has been placed on conductive indium tin oxide (ITO) glass and covered with a chemical matrix. The selected positions form a rectangular array of points at a chosen distance from each other, and a mass spectrum is collected at each location. This novel approach, called MALDI Imaging or MSI, is described schematically in Figure 1. With the addition of automation to the MALDI instruments (Stoeckli et al., 1999) and the development of new imaging software (Stoeckli et al., 2001), it is now possible to obtain maps showing the abundance of hundreds of individual biomolecules in tissue slices (Caprioli et al., 1997; Fournier et al., 2003; Chaurand et al., 2005, 2006a; Woods and Jackson, 2006; Jackson et al., 2007; Wang et al., 2007). Moreover, MALDI ion sources can be adapted to give access to different families of biomolecules, ranging from peptides and proteins to oligonucleotides, sugars, or lipids, with a spatial resolution at the cellular and potentially even at the subcellular levels.

MSI was first introduced by Caprioli and colleagues nearly a decade ago (Caprioli et al., 1997; Chaurand et al., 1999, 2002, 2006a,b), but it is still under active development in several laboratories seeking to design new instruments and to improve methods, such as sample preparation and spatial resolution, as well as identifying new applications, such as studies of tissue localization of drugs, biomarker discovery, or understanding molecular mechanisms (Stoeckli et al., 2002; Jackson et al., 2005a,b; Rohner et al., 2005; Rubakhin et al., 2005; Crossman et al., 2006; Hsieh et al., 2006, 2007; Roy et al., 2006; Stoeckli et al., 2006; Sugiura et al., 2006; Woods and Jackson, 2006; Chaurand et al., 2007; Jackson et al., 2007; McDonnell and Heeren, 2007; Reyzer and Caprioli, 2007; Shimma et al., 2007; Touboul et al., 2007).

In our group in Lille, we have focused our attention on different areas, such as tissue preparation, matrix deposition, laser focusing and, perhaps most importantly, on attaining a better understanding of the desorption/ionization process itself, since currently only $\sim$10% of the ions from the analyte arrive

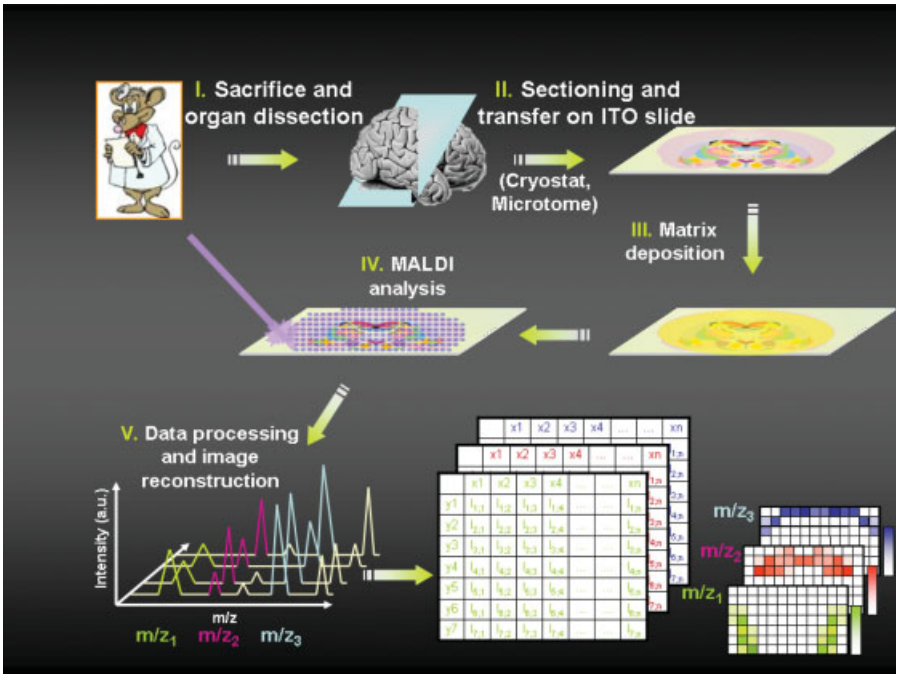

Figure 1 Schematic representation of MALDI imaging procedures. Tissue sections from fresh organ or biopsy are transferred onto an ITO glass slide. Sections are then covered with a specific matrix, depending on the nature of the biomolecule under study. For peptides/proteins, very intense signals are obtained with α-cyano-4-hydroxycinnamic acid (α-CHCA) as a matrix. Once the sections are covered with α-CHCA (or another matrix), the target is introduced in the MALDI-TOF instrument for analysis. Next, the MALDI laser scans through a set of preselected locations (10–50 μm apart) in the tissue and mass spectra representative of the peptides/proteins (or lipids) present at each location are collected. Automated data collection takes 2–6 h, depending on the number of points assayed, and followed by analysis and image reconstruction using imaging software. a.u., arbitrary units.

at the detector, making the technique less efficient than desirable for detecting low abundance species. Recent improvements include the identification of new solvent treatments that make possible MSI of long-stored frozen and paraffin-embedded tissues (Lemaire et al., 2006a,b), as well as novel ionic matrices that increase the sensitivity, the stability under vacuum and the yield per laser shot (Lemaire et al., 2006c). For formalin-fixed and paraffin-embedded (FFPE) tissue, microspotting with an enzyme and reactive matrices was developed (see Fig. 2) (Lemaire et al., 2007a). To increase sensitivity, gold sputtering on tissue slices has been assayed (Altelaar et al., 2006; Wisztorski et al., 2006). Another improvement developed by our team employs a silicon wafer mask to reduce the irradiated area to less than $30 \times 30\ \mu m^2$, without loss of signal intensity (Wisztorski et al., 2007b). Cellular level resolution can begin to be attained with MSI instruments equipped with these modifications. A new technique that will extend the range of molecules that can be mapped by MSI to nucleic acids and very large proteins was reported recently by our group (Lemaire et al., 2007b). This technique consists of tagging a molecular probe that binds specifically to a molecule of interest (e.g., a polynucleotide that hybridizes with a particular mRNA) with an identifying artificial peptide (the TAG) by means of a UV-photocleavable group. The MALDI UV laser can then be used to cleave the TAG, which is subsequently identified and localized by MSI, thus indirectly analyzing the distribution of the molecule of interest. Any number of TAGs of different mass can be used simultaneously with this approach, thus concurrently imaging the corresponding molecules of interest. Other important future advances will include the implementation of quantitative analysis and in tissue *de novo* sequencing, as well as improving the detection of proteins present at low concentration, a step that will require a better understanding of how to increase the efficiency of the desorption/ionization processes. Fundamental studies have to be undertaken to achieve all of these useful technical enhancements.

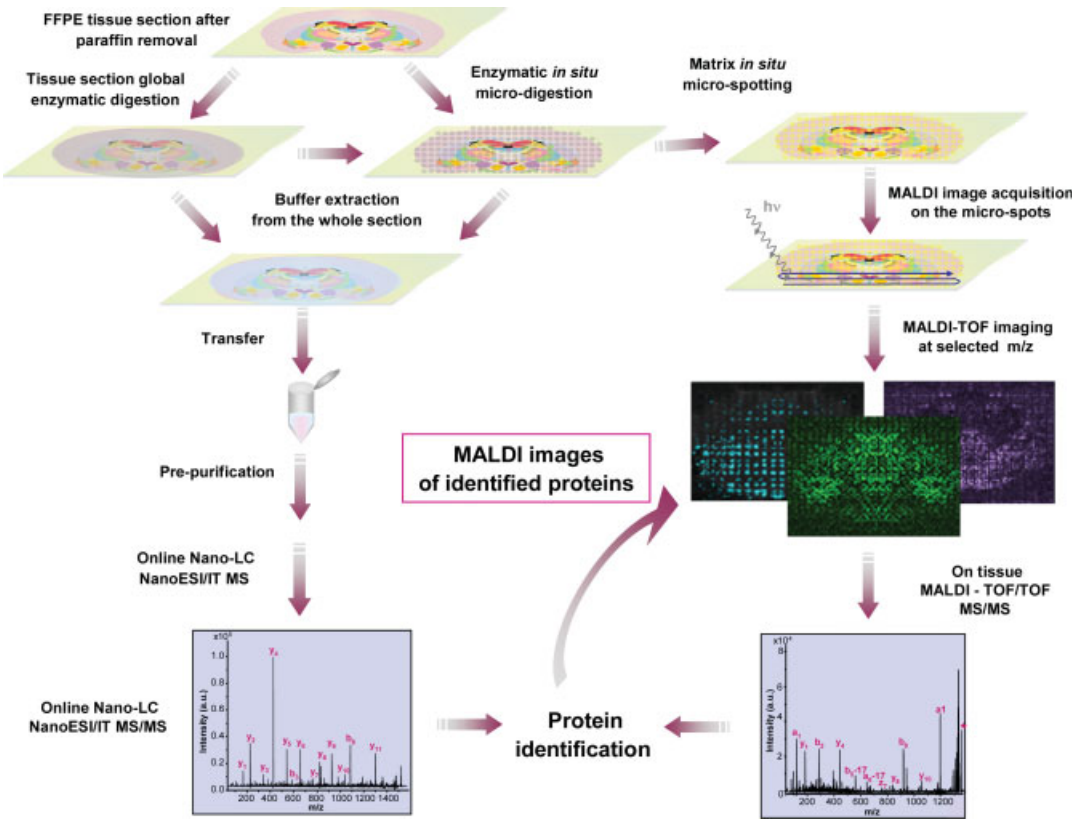

Figure 2 Strategies for identifying and imaging peptides or proteins from preserved tissue. Schematic diagram of protocols used to obtain molecular images as well as to identify proteins in FFPE (formalin-fixed and paraffin-embedded) tissues sections. These protocols have been successfully carried out even after lengthy tissue storage. As shown on the top row, trypsin microdigestion is performed on a tissue section prior to matrix microspotting and MALDI imaging. To identify proteins, adjacent sections are either globally digested or microdigested and extracted on the slide, transferred to an Eppendorf tube and purified, followed by nanoLC-nanoESI/IT and MS/MS analyses. Ions detected in the nanoLC ESI/IT analyses are then selected from the MALDI images for further study. With permission from Journal of Proteome Research (Lemaire et al., 2007a).

MSI can provide new directions for clinical proteomic studies, especially in the Neurosciences, with the joint goals of characterizing cellular circuitry and understanding the impact of disease and therapy on cellular networks through the analysis of pathological tissue samples (Wisztorski et al., 2007a). Of particular relevance to the focus of this special issue of Developmental Neurobiology, MSI has already been demonstrated to be a valuable technique for exploring the molecular components of neural structures, as discussed in the next two sections.

VERTEBRATE BRAIN STUDIES WITH MALDI MSI

Because its anatomy has been extensively characterized, the rat brain was the first biological model used in MALDI MSI studies, and several molecular maps of different neuropeptides have been reported (Fig. 3) (Jespersen et al., 1999; Fournier et al., 2003). These maps match accurately the corresponding distributions obtained using immunocytochemistry, but are not restricted to only those molecules for which antibodies are available. In fact, more than a thousand molecules can be detected in a single study. Beside peptides and proteins, molecular distributions of different classes of lipids have been mapped using MALDI MSI (Jackson et al., 2005a, 2007). MALDI MSI has also been used in differential display studies of animals injected with lipopolysaccharides (LPS) in order to mimic bacterial challenges. The presence of vasopressin in the supraoptic nucleus before LPS injection, and its decrease afterward, confirm the feasibility of accessing such information by MALDI MS profiling (Fournier et al., 2003).

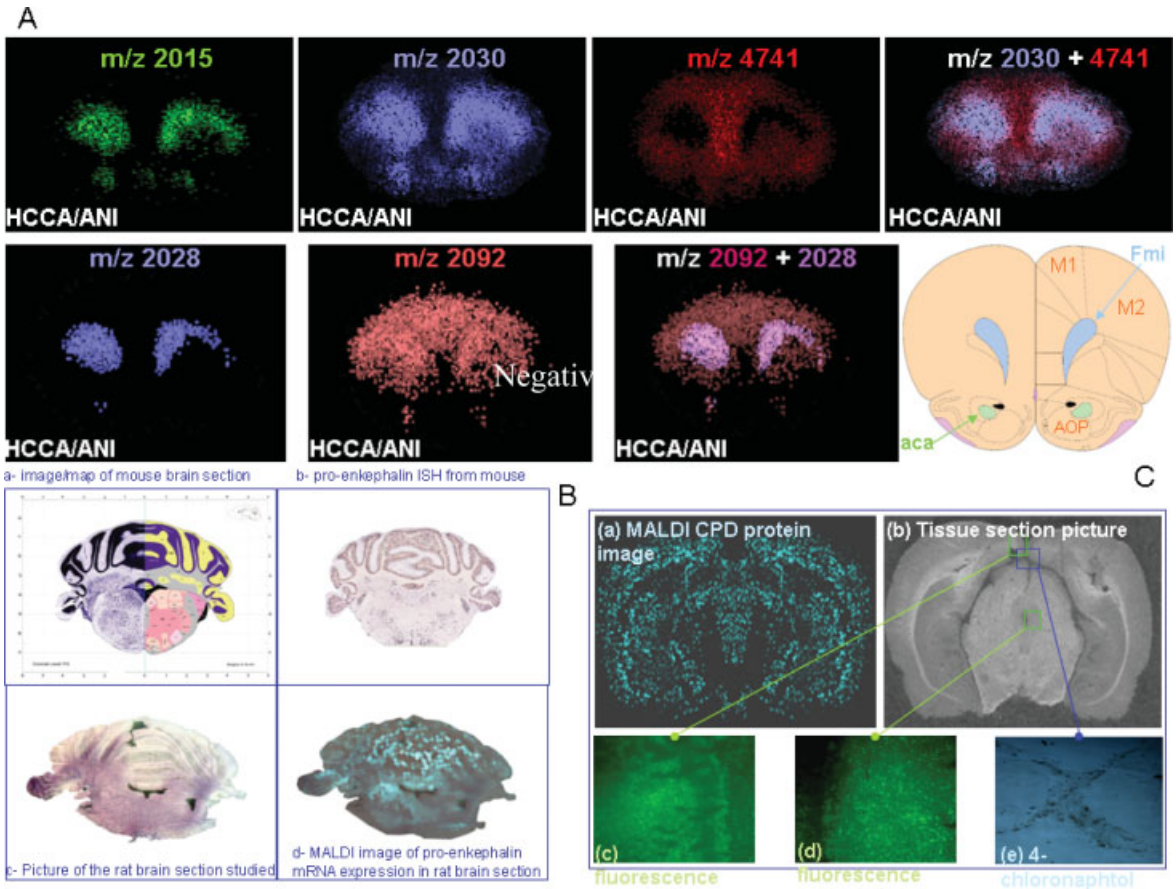

Figure 3 MALDI Imaging analysis of rodent brain slices. (A) MSI using MALDI TOF-TOF in reflector mode at 50-Hz repetition rate with ionic matrices CHCA/ANI in positive and negative modes. MALDI imaging can be compared with rat brain anatomy. Acquisitions in both polarities were performed on the same rat brain cut. Images have been reconstructed with the same parameters for ionic matrix using FlexImaging software and each represents the distribution of one value of *m*/*z* (noted) in the tissue slice. Images with two colors correspond to the superposition of two *m*/*z* images With permission from Analytical Chemistry (Lemaire et al., 2006c, 2007a,b). (B) Pro-enkephalin mRNA localization in 8-week-old male C57BL/6J mouse brain using digoxigenin ISH technique; from the Allen Institute Brain Atlas (http://www.brainatlas.org/aba/). Colorimetric detection of bound probe is generated by the alkaline phosphatase substrates nitroblue tetrazolium (NBT) and 5-bromo-4-chloro-3-indolyl phosphate (BCIP), which produce a vivid blue/purple particulate reaction product. (c) Picture of a rat brain slice before ISH with the U-tagged pro-enkephalin probe (d) MALDI molecular image reconstructed by scanning the tissue section after ISH experiment with the U-tagged pro-enkephalin probe (7000 spots, 100 μm from each other). (C) Rat brain tissue section picture before the ICC experiment and corresponding MALDI molecular image reconstructed on the tag peptide characteristic ion screening after ICC experiment with the tagged secondary antibody (30,000 spots separated each of 100 μm) (a,b) and comparison to pictures of specific region of the adjacent rat brain sections after ICC experiment with FITC (c,d) or peroxydase (e) secondary antibody.

In the case of pathologies produced by neurodegenerative diseases, MALDI MSI can yield novel information. Neurodegeneration induces various changes in the brain that may be investigated using neuroimaging techniques. The *in vivo* techniques are useful in the visualization of major changes, and in following the progressing abnormalities longitudinally. However, to study and quantify minor abnormalities, analysis of postmortem brain tissue is necessary (Langstrom et al., 2007). MSI techniques, for example, have been used to compare molecular patterns in prelesion and postlesion areas in different animal models of progressive Parkinson's Disease (PD) (Pierson et al., 2004). Protein patterns in the affected

brains are complex, and new molecular tools are needed to identify not only the changes in these patterns but also to identify the specific proteins involved. For instance, MS has been used to generate peptide and protein profiles of brain tissue sections obtained from rats administered with 6-hydroxydopamine (6-OHDA) unilaterally. Several differences were found in the dopamine-depleted side of the rat brain when compared to the corresponding intact side, in calmodulin, cytochrome c, and cytochrome c oxidase, for example, implicating denervation of dopamine neurons *per se* in the regulation of ubiquitin pathways, at least in a classical animal model of PD (Pierson et al., 2005). This study also emphasizes the utility of molecular profiling with MSI, because it has the capacity to distinguish between metabolic fragments, conjugated proteins, and posttranslational modifications (Pierson et al., 2005). Most antibodies used in immunocytochemical studies for assessing the presence of ubiquitin in PD-associated Lewy bodies are directed toward a protein-bound form of ubiquitin. Free monomeric ubiquitin is not immunogenic in most mammalian species used to produce antibodies (Pierson et al., 2005; Langstrom et al., 2007). These antibodies are also capable of cross-reacting with free monomeric ubiquitin, and therefore it is unclear in which form ubiquitin is detected using these immunocytochemical techniques. MSI, by comparison, easily discriminates between these two forms (Langstrom et al., 2007).

Recently, we examined MALDI tissue profiling combining the use of automatic spotting of MALDI matrix with *in situ* tissue enzymatic digestion of FFPE brain of 6-OHDA unilaterally treated animals (Lemaire et al., 2006a). The identification of compounds was carried out on adjacent sections by *in situ* tissue digestion followed by nanoLC/MS-MS analysis (Fig. 2). These analyses confirmed that ubiquitin, trans-elongation factor 1, hexokinase, and Neurofilament M are downregulated, as previously shown in both human and animal model tissues, whereas peroxidoredoxin 6, F1 ATPase and α-enolase are upregulated (Stauber et al., 2007). In addition, we identified three novel putative biomarkers, Trans elongation factor 1 (eEF1) and the collapsin response mediator proteins (CRMP-1 and -2) using protein libraries (Stauber et al., 2007). Our observation of increases in CRMP-1 and CRMP-2 is in agreement with previous molecular data (Barzilai et al., 2000). In Alzheimer's disease (AD), CRMP-2 has been implicated in neurite degeneration, acting on the assembly and polymerization of microtubules (Gu et al., 2000). Accumulation of Sema3A overlaps with the appearance of phosphorylated MAP1B and tau in many neurons, suggesting that Sema3A signaling at some level may be coupled to these previously identified cytoskeletal markers of neurodegeneration (Gu et al., 2000). The hippocampus of patients with AD expresses phosphorylated MAP1B, CRMP-2, Plexins A1 and A2, and a processed form of Sema3A (Gu et al., 2000).

To gain further insight into possible functions of CRMP-2, we recently applied MSI to sections of 6-OHDA treated rat brains to assess the distribution of CRMP-2 following induced neurodegeneration. Several examples of MALDI molecular images obtained from one such section are shown in Figure 4, for a selected set of ions corresponding to different digestion fragments of CRMP-2 (panels A–C). As a summary view, panel 4D displays the summed data for all those ions identified as digestion fragments of CRMP2. As would be expected for fragments from the same molecule, the distributions of the individual ions appears, despite some variation in image contrast, to be essentially the same (cf. panels 4A, 4B, and 4C to panel D). A striking feature of the distribution of CRMP-2 thus obtained is the clear localization of the protein to very specific regions of the brain. Interestingly, it is especially abundant in the *corpus callosum*, an area of the brain where CRMP-2 is not normally detected in the adult rat. This observation is not surprising, given that the *corpus callosum* has been implicated in dementia and many neurodegenerative diseases.

Along this line, Stoeckli's group has employed MSI in studies of amyloid β peptide distribution in mouse brain sections (Stoeckli et al., 2002, 2006). They distinguished three main regions, two showing abundant expression in the parietal and the occipital cortical lobes, and a third one close to the lower part of the Sylvian fissure, that is, in the hippocampus. The normalized distributions of Aβ-(1–40) and Aβ-(1–42) show that they are the most abundant amyloid peptides. MSI gives access to the levels of known targets, but also allows the mapping of the different targets with great accuracy, which is not possible when whole-brain extracts are analyzed (Stoeckli et al., 2002, 2006). These and other results mentioned above establish the great potential of MALDI MSI as a new tool for the study of the consequences of neurodegenerative disease.

MALDI MSI is also a very appropriate tool for assaying the distribution of pharmaceuticals in rat brain tissue slices, which is critical information for new drug development. In fact, some studies of clozapine (Hsieh et al., 2006) and repiridone (O'Brien et al., 2006) have recently been performed by MALDI MSI. The data confirm that chronic risperidone treatment, which is accompanied by a behavioral pheno-

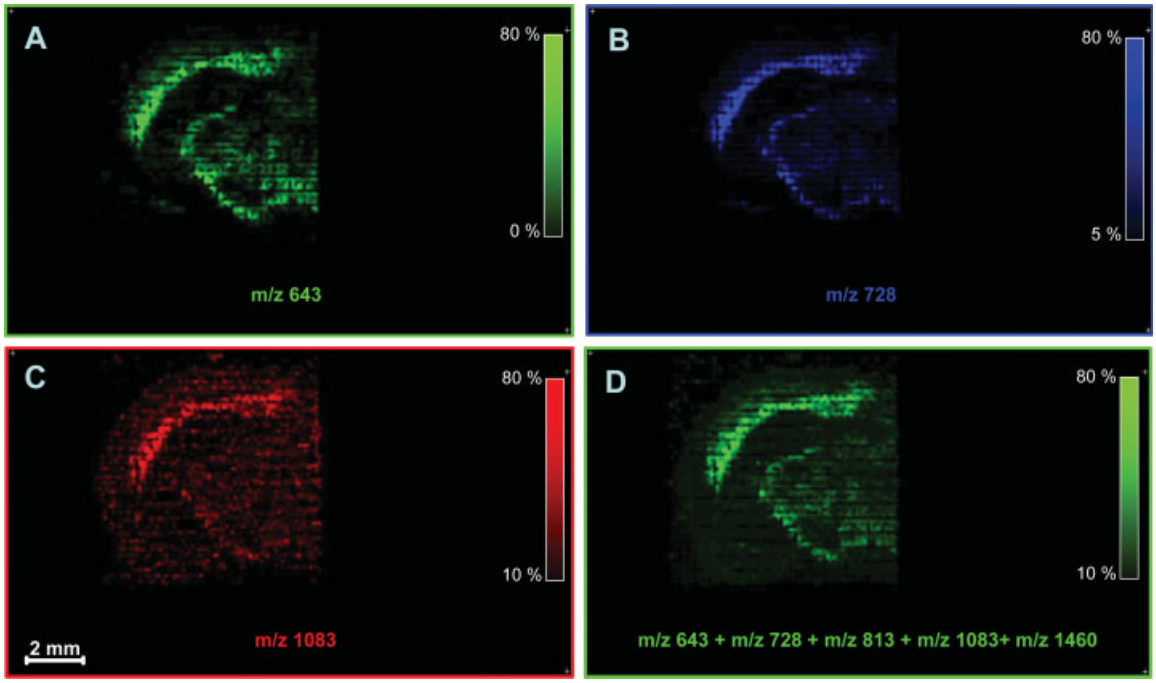

Figure 4 Detection of CRMP-2 protein with MALDI imaging. Molecular images reconstructed from MALDI MS data acquired from a section of a 6-OHDA-treated rat brain that had been stored after formalin fixation and paraffin embedding for over 9 years. The MS data was collected following *in situ* automatic spot trypsin digestion of the sectioned tissue. (A–C) Images of three individual ions corresponding to digestion fragments of CRMP-2 of *m/z* values equal to 643, 728, and 1083; (D) Composite image integrating the data on all ions identified as digestion fragments of the CRMP-2 protein.

type of extrapyramidal origin, produces alterations in the striatal protein profile, possibly subsequent to blockade of dopaminergic systems. These results suggest that possible mechanisms involved in antipsychotic-drug-induced extrapyramidal syndromes (APD-induced EPS) include metabolic dysfunction and oxidative stress (O'Brien et al., 2006).

INVERTEBRATE NERVOUS SYSTEM STUDIES USING MSI

Invertebrate nervous systems are also very well-suited to the application of MSI. For example, neuronal somata are often quite large (up to a millimeter in diameter in the mollusc *Aplysia*), neurons can be reliably identified and repeatedly studied in different experimental contexts, neural functions are frequently segregated in separate ganglia or regions of ganglia, and neural tissues can be readily and quickly prepared for study in a MALDI Imaging instrument (Garden et al., 1998; Li et al., 1998, 1999, 2000b; Painter et al., 1998; Rubakhin et al., 1999, 2000; Sweedler et al., 2000, 2002; Furukawa et al., 2001; Kruse et al., 2001; Schein et al., 2001). MSI studies complement, more traditional studies of peptides and proteins purified from selected regions of the invertebrate nervous system, and can be carried out in developing stages to obtain 4D (spatial + temporal) maps of specific molecules of interest. This level of analysis can be extended to studies of degeneration, regeneration and repair (Kruse and Sweedler, 2003).

The earliest peptide profiling experiments on invertebrate nervous systems using MALDI-MS were carried out on mollusks, first on the gastropod *Lymnaea stagnalis* (Jimenez et al., 1994, 1998; Li et al., 1994b, 2000a) and later on several cephalopods (Sweedler et al., 2000). The experimental strategy in these studies was the comparison of peptide mass spectra patterns obtained from different parts of the nervous system, for example, neuronal somata vs. neurohemal organ axon terminals (Jimenez et al., 1994; Li et al., 1994a,b). This approach resulted in the detection of novel peptides, in addition to peptides previously identified by conventional molecular biological and peptide chemistry methods. In this manner, complex peptide processing and expression patterns could be predicted that were not detected with more conventional methods.

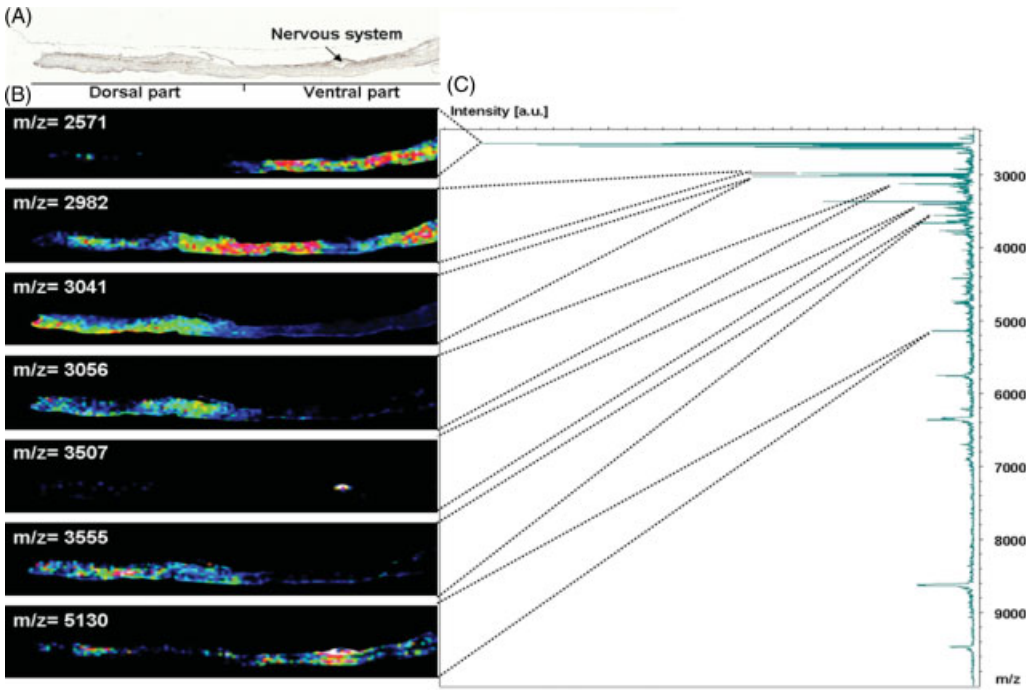

Figure 5 MALDI imaging of a transverse section of the body wall of an adult leech. The specimen was opened along the dorsal midline, pinned flat, exposed for ~2 min to methanol to harden the tissues, frozen and sectioned (12 μm-thickness) transversely. Sections were mounted on a metal-coated glass slide and imaged prior to being sprayed with CHCA matrix for MALDI analysis. (A) Low magnification, transmitted light digital image of a part of a transverse section, extending from the dorsal midline on the left (Dorsal part), through the ventral midline (Nervous system) and including the ventral region on the other side (Ventral part). Tissue dimensions ~0.5 mm × 14 mm. (B) MALDI images of the partial transverse section shown in a), reconstructed from mass spectra recorded in a raster of 2000 points, 100 μm apart. Seven *m*/*z* values are shown, illustrating some of the different molecular distributions observed. (C) Example of a mass spectrum obtained at one location, indicating the peaks corresponding to the *m*/*z* values of the MALDI images shown in B). Relative abundances are color coded, with red-white being high and blue-black low; a.u., arbitrary units. (M. Wisztorski, I. Fournier, M. Salzet and E. Macagno, unpublished results).

Such a strategy, combining peptide fingerprinting of single neurons by MALDI, molecular cloning, peptide chemistry, and electrospray ionization MS, has been generalized to study the intricate processing pattern of a preprohormone expressed in identified neurons. In *L. stagnalis*, some experiments were conducted on neuroendocrine light yellow cells (LYCs) or caudodorsal cells. The LYCs are known to express a precursor, named prepro-LYCP (LYCPs, light yellow cell peptides). Prediction of its processing into three peptides, LYCP I, II, and III, at conventional dibasic processing sites flanking the peptide domains on the precursor, were confirmed by MS. However, MALDI of single LYCs revealed trimmed variant peptides derived from LYCP I and II. The variants were much more abundant than the intact peptides, indicating that LYCP I and II serve as intermediates in a peptide-processing sequence (Li et al., 1994b). Furthermore, MALDI also allows detecting colocalization of a novel peptides with the LYCPs (Li et al., 1994b). Caudodorsal cells of Lymnaea are known to initiate and coordinate ovulation and egg mass production and associated behaviors through the release of a complex set of peptides that are derived from the caudodorsal cell hormone-I (CDCH-I) precursor. Fingerprinting by MALDI of peptides in the commissure demonstrated the presence of all sequenced peptides and, in addition, could identify two other peptides derived from pro-CDCH-1, the β 1-, and β 3-peptides. (Li et al., 1994a). Recently, Sweedler and colleagues, studying the bee *Apis mellifera* genome, showed that 200 neuropeptides can be predicted, of which 100 were confirmed by MS. Moreover, this study opens the door of future molecular studies with the identification of 36 genes, 33 of which were previously unreported (Hummon et al., 2006). Clearly,

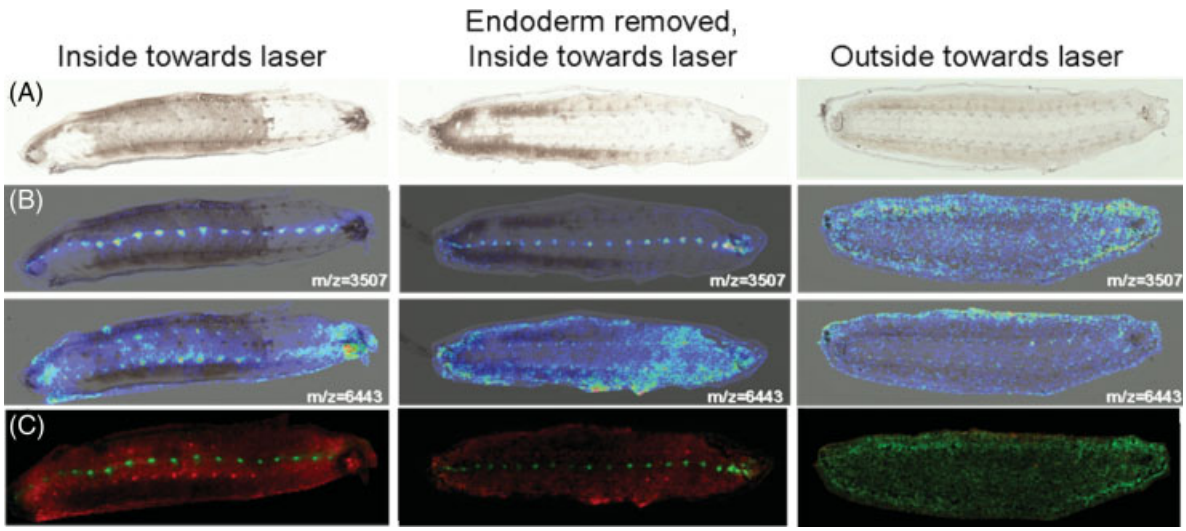

Figure 6 MALDI imaging of dissected leech embryos in whole mount. Three stage E12 specimens were opened along the dorsal midline and the yolk removed, then pinned flat, exposed for $\sim$2 min to methanol to harden the tissues, finally placed on metal-coated glass slides and immediately dried. MALDI images were reconstructed from the mass spectra collected from 20,000 locations covering the embryos completely in a rectangular raster of points 60 μm apart. (A) Transmitted light low-power micrographs of the unstained embryos (embryo dimensions $\sim$2.5 mm $\times$ 10 mm) taken prior to the spraying of CHCA matrix on the embryos for MALDI analysis. The embryo at left was mounted so the internal surface (endoderm) faced the laser beam, while the embryo in the middle was similarly prepared but the endodermal layer ($\sim$10 to 20-μm thick) was removed. The embryo at right was mounted with the epidermis toward the laser source. Anterior is to the right in all cases. (B) Recnstructed MALDI images showing the distributions of ions with m/z values of 3508 (above) and 6420 (below), for the three embryos. The 3507 ions are maximally present in the segmental ganglia and interganglionic connective nerves, in the two animals analyzed with the inner surface toward the laser. It is essentially absent in the third animal, as might be expected since the CNS is close to the inner surface, indicating that the depth range into the tissue of the laser beam is les than $\sim$100 μm. By contrast, the 6420 ion is more widely distributed but with maxima associated with the nephridiopores. Signal associated with the nephridiopores is visible in the specimen on the right column as well, presumably because these structures extend through the body wall and open to the outside. (C) Superposition of the images shown in (B), but here with abundance proportional to intensity in green (m/z = 3508) and red (m/z = 6420). (M. Wisztorski, I. Fournier, M. Salzet and E. Macagno, unpublished results).

MALDI peptide profiling gives access to the most complete peptide representation in specific areas, and differential analyses of several distinct areas with MSI yields a representative map of all biomolecules present at one time.

In another recent report, MSI of neuropeptides in crustacean neuronal tissues (pericardial organ and brain) was used to reveal that two RFamide-family peptides and a truncated orcokinin peptide map to locations distinct from those of other members of their respective families. Over 30 previously sequenced neuropeptides were identified based on mass measurement. MSI study at the organ-level study elucidated the spatial relationships between multiple neuropeptide isoforms of the same family as well as the relative distributions of neuropeptide families (Dekeyser et al., 2007).

We have recently begun a series of MALDI imaging studies of embryonic and adult medicinal leeches (Figs. 5 and 6). One of our goals is to test the possibility of obtaining molecular maps from whole mounted, opened embryos at different stages of development, in order to obtain maps of when and where specific proteins and peptides are first expressed and whether such expression is stable or variable in time and space. One particular goal is to identify the distribution of potential axon guidance or arbor boundary cues that may play critical roles in setting up sensory domains in the skin, a phenomenon known as tiling. Other projects include exploring changes in nervous system molecular expression patterns in response to systemic perturbations, such as mechanical trauma, which evokes a regenerative response, or septic shock, which

induces a neuronal innate immune response in these animals.

Our initial efforts included MSI tests in both adult and embryonic tissues. In the adult leech, sectioning of the much thicker tissues was essential, which was carried out in a cryostat microtome. For the example shown in Figure 5, an anaesthetized adult leech was opened and pinned flat, and transverse frozen sections mounted on a metal-coated glass slide and dried, photographed, and coated with matrix for MSI. Our interest here was to get a rough idea of the range of topographic distributions that could be visualized within the mass range of $\sim$1–15 kDa that can be recovered with the ionic matrix we employed. The histological image [Fig. 5(A)] shows a part of the body wall, extending from the dorsal midline on the left past the ventral midline, with the CNS indicated. Distributions of ions in the indicated peaks of the spectrum in panel (C) are shown in panel (B) of Figure 5. Interesting differences in localization are illustrated by these images. The ion *m*/*z* 2571 appears to be localized exclusively in ventral territory but absent from the nerve cord. The ion *m*/*z* 2982 appears to be distributed in a lateral region, including contiguous parts of both dorsal and ventral territories, and no presence in the area within and around the nervous system. Three ions were present in the dorsal part of the body wall, *m*/*z* 3041, *m*/*z* 3056, and *m*/*z* 3555, but differentially distributed within this region. The ion *m*/*z* 5130 was strongly localized in the nervous system and nearby, in a manner almost complementary to the ion *m*/*z* 2982. Last among these examples, the distribution of the ion *m*/*z* 3507 was the same as that observed in the embryo (see below), that is, present exclusively within the nervous system.

Figure 6 shows examples from several embryos at the E12 stage of development, opened and mounted either with the inside of the embryo or the epidermis facing the laser beam. In one case, the endodermal layer was removed during dissection. The embryos were dried on a slide covered with a thin, transparent metallic layer, and a histological image was recorded prior to covering the tissues with a layer of matrix.

Molecular images of different *m*/*z* values were reconstructed after data acquisition for each embryo. MSI images, superposed on the histological images, are shown for ions at *m*/*z* 3507 and *m*/*z* 6443 (Fig. 6). For example, for the two embryos imaged from the internal surface, the ion *m*/*z* 3507 was exclusively localized in the nervous system, in ganglia, interganglionic connective nerves and lateral roots, proximal to the ganglia. By contrast, the ion *m*/*z* 6443 was not detected in the nerve chord but in nephridial structures, probably around the nephridiopores. The composite image illustrates very well this difference of localization between the two molecules. In comparison, for the embryo positioned with the epidermis toward the laser beam (right side in Fig. 6), no significant signal was observed for the *m*/*z* 3507 ion, confirming its localization to the internal CNS, while a reduced but detectable signal for the *m*/*z* 6443 ion was observed at the nephridiopores, which travel through the body wall and open to the outside in the epidermis. These very preliminary results demonstrate the possibility of using MSI to obtain whole embryo molecular maps, with reasonable resolution; though a careful exploration of methods for obtaining depth information will be necessary.

Although our studies of the leech embryo and adult are clearly at a very early stage, and much needs to be done to identify the molecules represented by each peak of interest in the mass spectra, to assay the actual volume being imaged at each point and to extend the resolution to the cellular and subcellular levels, it is already apparent that much can be learned by applying MSI to this preparation. While the identity (or amino acid sequence) of the molecule or molecules represented by each peak in the mass spectra is presently unknown, some types of questions can begin to be explored without prior knowledge of these identities. For example, we can determine all *m*/*z* values that are expressed exclusively in the CNS and then ask whether some are more strongly expressed in some segments than others, or if some are expressed at different developmental stages, or whether some change expression levels as a result of specific perturbations. Once we have selected those *m*/*z* values that fit our criteria, then the more arduous job of finding their molecular identities can be undertaken, but on a much reduced set of possibilities than going after every peak in the spectrum.

In combination with classical biochemical methods, MS has been largely responsible for revealing the richness of the expanded biological diversity at the protein level, due to alternative splicing and post-translational modifications that could not have been easily predicted from genomic sequence databases. MSI applied to invertebrate nervous systems, those discussed here and many others, has much to contribute to the elucidation of molecular mechanisms underlying dynamic processes, including development, maintenance, and repair.

CONCLUSIONS

Identification of all the relevant molecular components is a critical contribution to the search for the

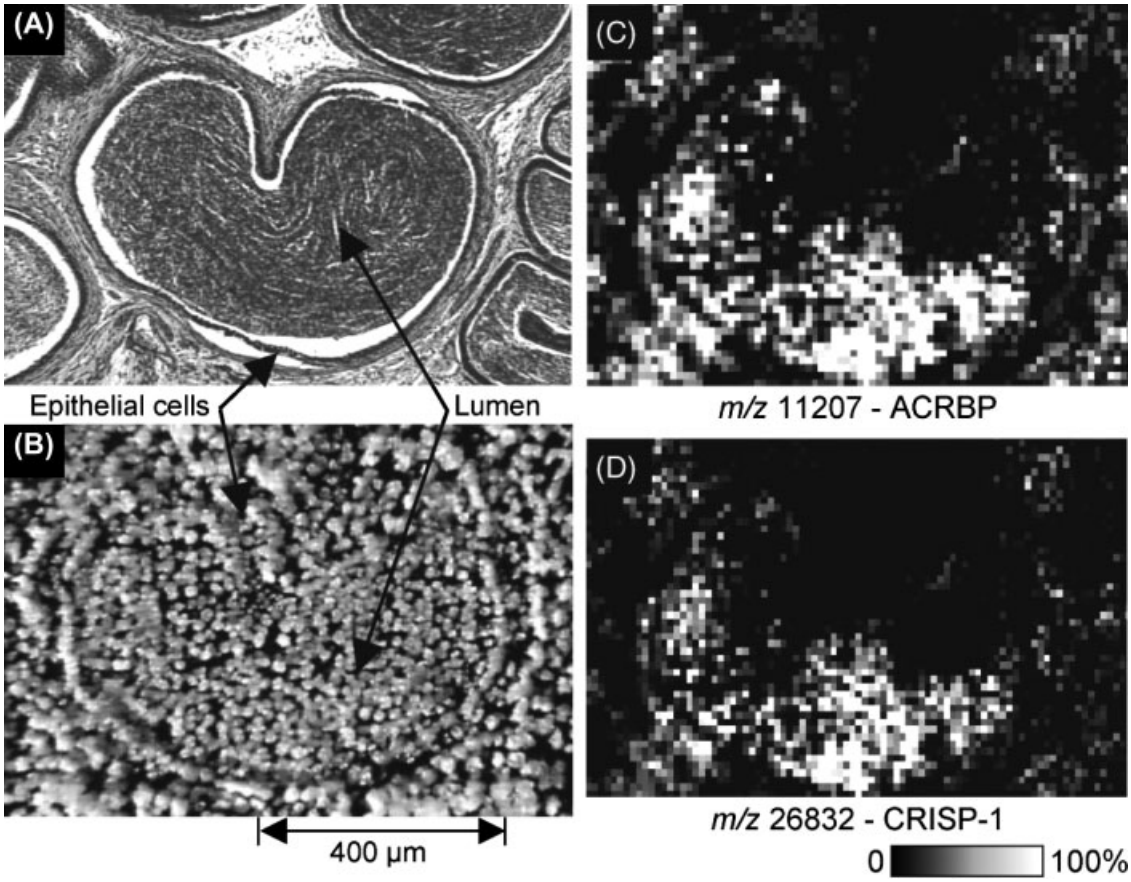

Figure 7 Cellular level resolution MALDI-MS imaging of tissue sections. Novel MALDI-MS imaging instrument designs by Caprioli and collaborators (Chaurand et al., 2007) can achieve resolutions in tissue sections of the order of 10 μm. Panels (A) and (B) show photomicrographs of a 12 μm section of mouse cauda epididymis tissue before and after ionic matrix deposition, respectively, and prior to IMS analysis. A tubule is indicated by the arrows pointing at the layer of Epithelial cells and the Lumen. Panels (C) and (D) show ion density maps within the lumen of the tubule shown in (A), corresponding to two secreted epididymal proteins, proacrosin binding protein (ACRBP, m/z = 11,207) and cysteine-rich secreted protein-1 (CRISP-1, m/z = 26,832), derived from the mass spectra acquired with a focused laser beam ($\sim$7 μm diam.). The resolution is of the order of 10 μm. (Modified from Chaurand et al., 2007).

mechanisms responsible for specific neural functions and for the changes brought about by traumatic perturbations or disease. In many instances, key molecules have been identified and tested, and increasingly their participation observed dynamically by detecting them with several different techniques. However, it is possible, if not probable, that unknown factors are also contributing to the phenomena under study, which need to be identified and included as well. A range of powerful MS techniques, together with the amino acid sequences predicted from expression analysis of genomic and transcriptomic sequence databases, are an effective means for identifying, characterizing, and quantifying both known and novel proteins and peptides present in the neural tissue under study. The enhancement of the MALDI MS technique by the addition of a scanning capability, as discussed in this review, yields additional information about the distribution and abundance of each detected peptide or protein in specific tissues and locations, information that may also provide clues about their potential functional roles. While the currently available instruments and techniques for MSI are quite useful in this respect, several groups are pursuing improvements that will significantly expand its capabilities. For example, on-going efforts to improve MALDI MSI instrument design in order to achieve resolutions below 10 μm (e.g., Chaurand et al., 2007; see Fig. 7) will extend the range of questions that can be approached with this technique to individual cells

and to the subcellular level, and therefore to many important questions about neuronal function that require these levels of detail.

Several current applications of MALDI Imaging, or MSI, were discussed here, and many other possibilities come to mind. For instance, compared to the dynamic imaging techniques reviewed in other contributions to this issue of Developmental Neurobiology, MSI presently can only provide snapshots of the molecular components present at specific times within an experimental paradigm, and not a real-time sequence of observations. One strategy, however, might be to couple dynamic functional imaging of tissue slices with MSI snapshots at selected critical times, which would yield unique and much more complete information about which molecules are present and could contribute to the mechanisms underlying the phenomena under study.

REFERENCES

Aebersold R, Goodlett DR. 2001. Mass spectrometry in proteomics. Chem Rev 101:269–295.

Altelaar AF, Klinkert I, Jalink K, de Lange RP, Adan RA, Heeren RM, Piersma SR. 2006. Gold-enhanced biomolecular surface imaging of cells and tissue by SIMS and MALDI mass spectrometry. Anal Chem 78:734–742.

Barzilai A, Zilkha-Falb R, Daily D, Stern N, Offen D, Ziv I, Melamed E, et al. 2000. The molecular mechanism of dopamine-induced apoptosis: Identification and characterization of genes that mediate dopamine toxicity. J Neural Transm Suppl 60:59–76.

Caprioli RM, Farmer TB, Gile J. 1997. Molecular imaging of biological samples: Localization of peptides and proteins using MALDI-TOF MS. Anal Chem 69:4751–4760.

Chaurand P, Cornett DS, Caprioli RM. 2006a. Molecular imaging of thin mammalian tissue sections by mass spectrometry. Curr Opin Biotechnol 17:431–436.

Chaurand P, Norris JL, Cornett DS, Mobley JA, Caprioli RM. 2006b. New developments in profiling and imaging of proteins from tissue sections by MALDI mass spectrometry. J Proteome Res 5:2889–2900.

Chaurand P, Schriver KE, Caprioli RM. 2007. Instrument design and characterization for high resolution MALDI-MS imaging of tissue sections. J Mass Spectrom 42:476–489.

Chaurand P, Schwartz SA, Caprioli RM. 2002. Imaging mass spectrometry: A new tool to investigate the spatial organization of peptides and proteins in mammalian tissue sections. Curr Opin Chem Biol 6:676–681.

Chaurand P, Schwartz SA, Reyzer ML, Caprioli RM. 2005. Imaging mass spectrometry: Principles and potentials. Toxicol Pathol 33:92–101.

Chaurand P, Stoeckli M, Caprioli RM. 1999. Direct profiling of proteins in biological tissue sections by MALDI mass spectrometry. Anal Chem 71:5263–5270.

Crossman L, McHugh NA, Hsieh Y, Korfmacher WA, Chen J. 2006. Investigation of the profiling depth in matrix-assisted laser desorption/ionization imaging mass spectrometry. Rapid Commun Mass Spectrom 20:284–290.

Dekeyser SS, Kutz-Naber KK, Schmidt JJ, Barrett-Wilt GA, Li L. 2007. Imaging mass spectrometry of neuropeptides in decapod crustacean neuronal tissues. J Proteome Res 6:1782–1791.

Fournier I, Day R, Salzet M. 2003. Direct analysis of neuropeptides by in situ MALDI-TOF mass spectrometry in the rat brain. Neuro Endocrinol Lett 24:9–14.

Furukawa Y, Nakamaru K, Wakayama H, Fujisawa Y, Minakata H, Ohta S, Morishita F, et al. 2001. The enterins: A novel family of neuropeptides isolated from the enteric nervous system and CNS of Aplysia. J Neurosci 21:8247–8261.

Garden RW, Shippy SA, Li L, Moroz TP, Sweedler JV. 1998. Proteolytic processing of the Aplysia egg-laying hormone prohormone. Proc Natl Acad Sci USA 95: 3972–3977.

Gu Y, Hamajima N, Ihara Y. 2000. Neurofibrillary tangle-associated collapsin response mediator protein-2 (CRMP-2) is highly phosphorylated on Thr-509, Ser-518, and Ser-522. Biochemistry 39:4267–4275.

Hsieh Y, Casale R, Fukuda E, Chen J, Knemeyer I, Wingate J, Morrison R, et al. 2006. Matrix-assisted laser desorption/ionization imaging mass spectrometry for direct measurement of clozapine in rat brain tissue. Rapid Commun Mass Spectrom 20:965–972.

Hsieh Y, Chen J, Korfmacher WA. 2007. Mapping pharmaceuticals in tissues using MALDI imaging mass spectrometry. J Pharmacol Toxicol Methods 55:193–200.

Hummon AB, Richmond TA, Verleyen P, Baggerman G, Huybrechts J, Ewing MA, Vierstraete E, et al. 2006. From the genome to the proteome: Uncovering peptides in the Apis brain. Science 314:647–649.

Jackson SN, Wang HY, Woods AS. 2005a. Direct profiling of lipid distribution in brain tissue using MALDI-TOFMS. Anal Chem 77:4523–4527.

Jackson SN, Wang HY, Woods AS. 2005b. In situ structural characterization of phosphatidylcholines in brain tissue using MALDI-MS/MS. J Am Soc Mass Spectrom 16:2052–2056.

Jackson SN, Wang HY, Woods AS. 2007. In situ structural characterization of glycerophospholipids and sulfatides in brain tissue using MALDI-MS/MS. J Am Soc Mass Spectrom 18:17–26.

Jespersen S, Chaurand P, van Strien FJ, Spengler B, van der Greef J. 1999. Direct sequencing of neuropeptides in biological tissue by MALDI-PSD mass spectrometry. Anal Chem 71:660–666.

Jimenez CR, Li KW, Dreisewerd K, Spijker S, Kingston R, Bateman RH, Burlingame AL, et al. 1998. Direct mass spectrometric peptide profiling and sequencing of single

neurons reveals differential peptide patterns in a small neuronal network. Biochemistry 37:2070–2076.

Jimenez CR, van Veelen PA, Li KW, Wildering WC, Geraerts WP, Tjaden UR, van der Greef J. 1994. Neuropeptide expression and processing as revealed by direct matrix-assisted laser desorption ionization mass spectrometry of single neurons. J Neurochem 62:404–407.

Kruse R, Sweedler JV. 2003. Spatial profiling invertebrate ganglia using MALDI MS. J Am Soc Mass Spectrom 14:752–759.

Kruse RA, Rubakhin SS, Romanova EV, Bohn PW, Sweedler JV. 2001. Direct assay of Aplysia tissues and cells with laser desorption/ionization mass spectrometry on porous silicon. J Mass Spectrom 36:1317–1322.

Langstrom B, Andren PE, Lindhe O, Svedberg M, Hall H. 2007. In vitro imaging techniques in neurodegenerative diseases. Mol Imaging Biol 9:161–175.

Lemaire R, Desmons A, Ducroy P, Tabet JC, Salzet M, Fournier I. 2006a. Direct analysis and MALDI imaging on formalin fixed paraffin embedded tissue (FFPE): Application to Parkinson disease. Proceedings of 54rd ASMS conference on Mass Spectrometry. Seattle, Washington, May 30–June 2.

Lemaire R, Desmons A, Tabet JC, Day R, Salzet M, Fournier I. 2007a. Direct analysis and MALDI imaging of formalin-fixed, paraffin-embedded tissue sections. J Proteome Res 6:1295–1305.

Lemaire R, Stauber J, Wisztorski M, Van Camp C, Desmons A, Deschamps M, Proess G, et al. 2007b. Tagmass: Specific molecular imaging of transcriptome and proteome by mass spectrometry based on photocleavable tag. J Proteome Res 6:2057–2067.

Lemaire R, Tabet JC, Ducoroy P, Hendra JB, Salzet M, Fournier I. 2006c. Solid ionic matrixes for direct tissue analysis and MALDI imaging. Anal Chem 78:809–819.

Lemaire R, Wisztorski M, Desmons A, Tabet JC, Day R, Salzet M, Fournier I. 2006b. MALDI-MS direct tissue analysis of proteins: Improving signal sensitivity using organic treatments. Anal Chem 78:7145–7153.

Li KW, Hoek RM, Smith F, Jimenez CR, van der Schors RC, van Veelen PA, Chen S, et al. 1994b. Direct peptide profiling by mass spectrometry of single identified neurons reveals complex neuropeptide-processing pattern. J Biol Chem 269:30288–30292.

Li KW, Jimenez CR, Van Veelen PA, Geraerts WP. 1994a. Processing and targeting of a molluscan egg-laying peptide prohormone as revealed by mass spectrometric peptide fingerprinting and peptide sequencing. Endocrinology 134:1812–1819.

Li L, Garden RW, Romanova EV, Sweedler JV. 1999. In situ sequencing of peptides from biological tissues and single cells using MALDI-PSD/CID analysis. Anal Chem 71:5451–5458.

Li L, Garden RW, Sweedler JV. 2000a. Single-cell MALDI: A new tool for direct peptide profiling. Trends Biotechnol 18:151–160.

Li L, Moroz TP, Garden RW, Floyd PD, Weiss KR, Sweedler JV. 1998. Mass spectrometric survey of interganglionically transported peptides in Aplysia. Peptides 19:1425–1433.

Li L, Romanova EV, Rubakhin SS, Alexeeva V, Weiss KR, Vilim FS, Sweedler JV. 2000b. Peptide profiling of cells with multiple gene products: Combining immunochemistry and MALDI mass spectrometry with on-plate microextraction. Anal Chem 72:3867–3874.

McDonnell LA, Heeren RM. 2007. Imaging mass spectrometry. Mass Spectrom Rev 26:606–643.

O'Brien E, Dedova I, Duffy L, Cordwell S, Karl T, Matsumoto I. 2006. Effects of chronic risperidone treatment on the striatal protein profiles in rats. Brain Res 1113:24–32.

Painter SD, Clough B, Garden RW, Sweedler JV, Nagle GT. 1998. Characterization of Aplysia attractin, the first water-borne peptide pheromone in invertebrates. Biol Bull 194:120–131.

Pierson J, Norris JL, Aerni HR, Svenningsson P, Caprioli RM, Andren PE. 2004. Molecular profiling of experimental Parkinson's disease: Direct analysis of peptides and proteins on brain tissue sections by MALDI mass spectrometry. J Proteome Res 3:289–295.

Pierson J, Svenningsson P, Caprioli RM, Andren PE. 2005. Increased levels of ubiquitin in the 6-OHDA-lesioned striatum of rats. J Proteome Res 4:223–226.

Reyzer ML, Caprioli RM. 2007. MALDI-MS-based imaging of small molecules and proteins in tissues. Curr Opin Chem Biol 11:29–35.

Rohner TC, Staab D, Stoeckli M. 2005. MALDI mass spectrometric imaging of biological tissue sections. Mech Ageing Dev 126:177–185.

Roy S, Touboul D, Brunelle A, Germain DP, Prognon P, Laprevote O, Chaminade P. 2006. [Imaging mass spectrometry: A new tool for the analysis of skin biopsy. Application in Fabry's disease]. Ann Pharm Fr 64:328–334.

Rubakhin SS, Garden RW, Fuller RR, Sweedler JV. 2000. Measuring the peptides in individual organelles with mass spectrometry. Nat Biotechnol 18:172–175.

Rubakhin SS, Jurchen JC, Monroe EB, Sweedler JV. 2005. Imaging mass spectrometry: Fundamentals and applications to drug discovery. Drug Discov Today 10:823–837.

Rubakhin SS, Li L, Moroz TP, Sweedler JV. 1999. Characterization of the Aplysia californica cerebral ganglion F cluster. J Neurophysiol 81:1251–1260.

Schein CH, Nagle GT, Page JS, Sweedler JV, Xu Y, Painter SD, Braun W. 2001. Aplysia attractin: Biophysical characterization and modeling of a water-borne pheromone. Biophys J 81:463–472.

Shimma S, Sugiura Y, Hayasaka T, Hoshikawa Y, Noda T, Setou M. 2007. MALDI-based imaging mass spectrometry revealed abnormal distribution of phospholipids in colon cancer liver metastasis. J Chromatogr B Analyt Technol Biomed Life Sci 855:98–103.

Stauber J, Lemaire R, Julien F, Bonnel D, Wisztorski M, Croix D, Fournier I, et al. 2007. Analysis of proteins in FFPE rat brain tissue sections from 6-OHDA treated animals by MALDI mass spectrometry. J Proteome Res, in press.

Stoeckli M, Chaurand P, Hallahan DE, Caprioli RM. 2001. Imaging mass spectrometry: A new technology for the analysis of protein expression in mammalian tissues. Nat Med 7:493–496.

Stoeckli M, Farmer TB, Caprioli RM. 1999. Automated mass spectrometry imaging with a matrix-assisted laser desorption ionization time-of-flight instrument. J Am Soc Mass Spectrom 10:67–71.

Stoeckli M, Knochenmuss R, McCombie G, Mueller D, Rohner T, Staab D, Wiederhold KH. 2006. MALDI MS imaging of amyloid. Methods Enzymol 412:94–106.

Stoeckli M, Staab D, Staufenbiel M, Wiederhold KH, Signor L. 2002. Molecular imaging of amyloid β peptides in mouse brain sections using mass spectrometry. Anal Biochem 311:33–39.

Sugiura Y, Shimma S, Setou M. 2006. Two-step matrix application technique to improve ionization efficiency for matrix-assisted laser desorption/ionization in imaging mass spectrometry. Anal Chem 78:8227–8235.

Sweedler JV, Li L, Floyd P, Gilly W. 2000. Mass spectrometric survey of peptides in cephalopods with an emphasis on the FMRFamide-related peptides. J Exp Biol 203:3565–3573.

Sweedler JV, Li L, Rubakhin SS, Alexeeva V, Dembrow NC, Dowling O, Jing J, et al. 2002. Identification and characterization of the feeding circuit-activating peptides, a novel neuropeptide family of aplysia. J Neurosci 22:7797–7808.

Touboul D, Brunelle A, Germain DP, Laprevote O. 2007. [A new imaging technique as a diagnostic tool: Mass spectrometry]. Presse Med 36 Spec No 1:1S82–S87.

Wang HY, Jackson SN, Woods AS. 2007. Direct MALDI-MS analysis of cardiolipin from rat organs sections. J Am Soc Mass Spectrom 18:567–577.

Wisztorski M, Brunet L, Dreiserwer K, Hillenkamp F, Berkenkamp S, Salzet M, Fournier I. 2006.Effect of metals coating for YV MALDI-a-TOF mass spectrometry imaging (MALDI MSI) and direct tissue analysis in UV/IR MALDI-o-TOF mass spctrometry. Proceedings of 54rd ASMS conference on Mass Spectrometry. Seattle, Washington, May 30–June 2.

Wisztorski M, Lemaire R, Stauber J, Ait Menguellet S, Jardin-Mathe O, Day R, Salzet M, et al. 2007a. [MALDI imaging: A new technology to discover and validate new biomarkers.]. Med Sci (Paris) 23:31–38.

Wisztorski M, Verplanck N, Thomy V, Stauber J, Camart JC, Salzet M, Fournier I. 2007b. Use of Masks in MALDI-MSI: An Easy Tool for Increasing Spatial Resolution of Images by Decreasing Irradiated Area. Indianapolis: American Society of mass spectrometry, June 4–7, 2007.

Woods AS, Jackson SN. 2006. Brain tissue lipidomics: Direct probing using matrix-assisted laser desorption/ionization mass spectrometry. AAPS J 8:E391–E395.